

B-4-1

Effects of Electron-Phonon Interaction on Transport Characteristics of Sub-10-nm Bulk-MOSFETs

Hiroshi Takeda and Nobuya Mori

Department of Electronic Engineering, Osaka University
2-1 Yamada-oka, Suita City, Osaka 565-0871, Japan
Tel: +81-6-6879-7767, Fax: +81-6-6879-7753
E-mail: takeda@ele.eng.osaka-u.ac.jp

1 Introduction

It has been clearly demonstrated that the direct source-to-drain (SD) tunneling current plays an important role in sub-10-nm planar bulk-MOSFETs even under the room-temperature operation [1]. To simulate the device characteristics of such ultra-small MOSFETs, full-quantum transport approach is, therefore, required. Moreover, at room temperature, the electron-phonon interaction becomes a dominant scattering mechanism, and it is important to study the effects of phonon scattering on the transport characteristics of sub-10-nm bulk-MOSFETs. In this paper, we have performed a quantum transport simulation based on a non-equilibrium Green's function (NEGF) method for sub-10-nm bulk-MOSFETs including the electron-phonon interaction, and investigated the phonon scattering effects on the transport characteristics.

2 Simulation Method

In our simulation, NEGF transport equations are solved self-consistently with the Poisson equation. A coupled mode-space method [2] is applied for solving the NEGF transport equations. In the coupled mode-space method, a real-space basis along the SD-direction and an eigen-mode basis along the gate-confinement direction are used for expanding the device Hamiltonian. Semi-infinite equilibrium reservoirs are assumed to be connected at the both ends of the source and drain regions. Fermi levels of the source and drain reservoirs are determined by the applied source and drain voltages. The electron-phonon interaction with a constant matrix element of $|M(q)|^2 = \hbar D^2 / 2\rho\omega_0$ is included within the self-consistent Born approximation [3]. Here D is the deformation potential, ρ is the density of the material, and ω_0 is the phonon frequency. We take both intra- and inter-subband scatterings into account in the simulation.

3 Results and Discussion

Figure 1 shows the simulated energy resolved electron-density distribution along the SD-direction of the "well-tempered" bulk-Si n -MOSFET [4] with 9 nm-gate-length for $V_g = 1.2$ V and $V_d = 0.5$ V at $T = 300$ K. The intra-valley phonon scattering with $\hbar\omega_0 = 61.2$ meV and $D = 11.0 \times 10^{10}$ eV/m is included. A mid-gap work function metal gate is assumed. The solid line indicates the low-

est subband energy profile along the SD-direction. We see that the electron-phonon interaction redistributes the electron density at the drain region. We also see that electrons exist in the energy region below the subband energy due to the polaronic effect [5].

Figure 2 illustrates the calculated I_d - V_g characteristics for $V_d = 0.5$ V at $T = 300$ K. $I_{\text{Ballistic}}$ is the drain current in the ballistic limit (closed circles) and I_{Phonon} is that with the electron-phonon interaction (open circles). In Fig. 2, we also plot the ratio of the SD tunneling current [6] to the total drain current. Comparing I_{Phonon} with $I_{\text{Ballistic}}$, we see that the effects of the electron-phonon interaction is more significant at the on-state. Figure 3 shows $I_{\text{Phonon}}/I_{\text{Ballistic}}$ as a function of V_g . $I_{\text{Phonon}}/I_{\text{Ballistic}}$ at $T = 300$ K (closed circles) is about 75 % at $V_g = 1.2$ V, while it is about 95 % at $V_g = -0.8$ V. In the case without the phonon absorption process (triangular symbols), I_{Phonon} decreases to about 50 % of $I_{\text{Ballistic}}$ at $V_g = -0.8$ V. These features can be explained by the fact that the phonon-assisted tunneling process enhances the tunneling probability and the SD tunneling current. Since the SD tunneling current dominates the device characteristics at the off-state as shown in Fig. 2, the increase in the tunneling current due to the phonon-assisted process

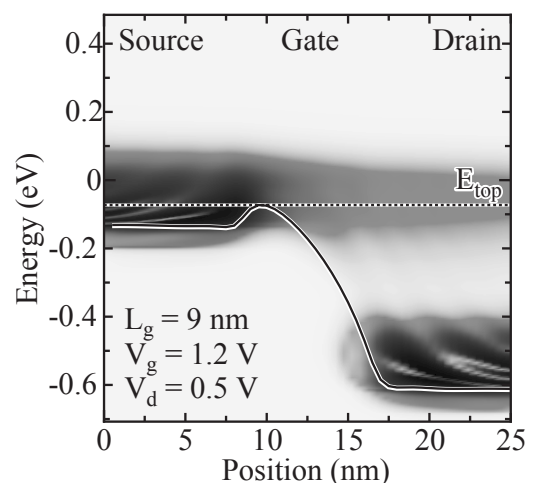


Figure 1: Energy resolved electron-density distribution along the SD-direction of the 9 nm-gate-length MOSFET. Solid line indicates the subband energy profile.

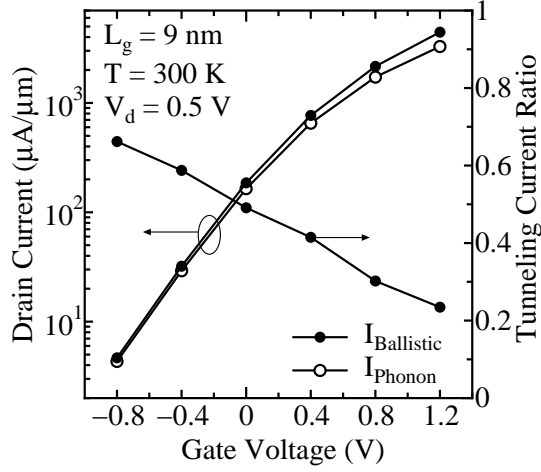


Figure 2: I_d - V_g characteristics and the SD tunneling current ratio of the 9 nm-gate-length MOSFET for $V_d = 0.5$ V at $T = 300$ K. Closed and open circles represent the results without and with the electron-phonon interaction, respectively.

mainly affects the off-current. As a result, the electron-phonon interaction degrades not only the on-current but also the subthreshold characteristics at the room-temperature.

Under the low-temperature operation, the degradation of the subthreshold characteristics due to the phonon assisted tunneling is expected to be suppressed. We have simulated the low-temperature characteristics of the 9 nm-gate-length MOSFET. In Fig. 3, $I_{\text{Phonon}}/I_{\text{Ballistic}}$ at $T = 30$ K is plotted by open circles. Figure 4 shows the average electron energy in the drain current, E_J^{avg} , and the maximum channel barrier height of the lowest subband, E_{top} , at $T = 300$ K (closed circles) and at 30 K (open circles). At $T = 300$ K, E_J^{avg} increases as V_g decreases, which results in the strong phonon emission and the reduction of the drain current at the off-state (this reduction will be compensated by the phonon-assisted process). On the other hand, at $T = 30$ K, since E_J^{avg} varies little in the off-state region and there is little source injection above the source Fermi level ($E_f^S = 0$ eV), the electron-phonon interaction plays a minor role and the reduction of the drain current due to the phonon emission is small at the off-state. However, at the on-state, E_J^{avg} becomes higher than E_{top} and the phonon emission processes again reduce the on-current even at $T = 30$ K.

4 Conclusions

Quantum transport simulation based on the NEGF method have been performed for sub-10-nm planar bulk-MOSFETs including the electron-phonon interaction. Simulation results show that the electron-phonon interaction reduces mainly the on-current rather than the off-current not only at room temperature but also at low temperature.

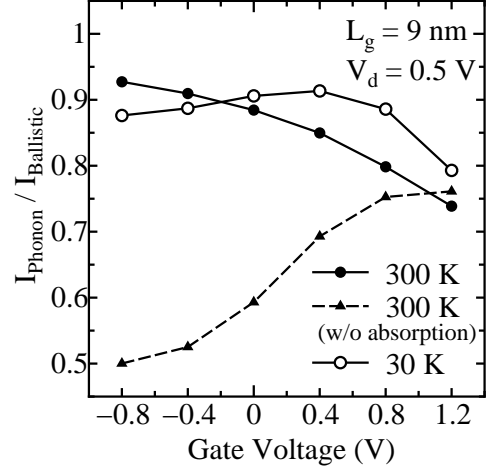


Figure 3: V_g dependence of $I_{\text{Phonon}}/I_{\text{Ballistic}}$ at $T = 300$ K (closed circles) and at $T = 30$ K (open circles). Triangular symbols represent the result without the phonon-absorption process at $T = 300$ K.

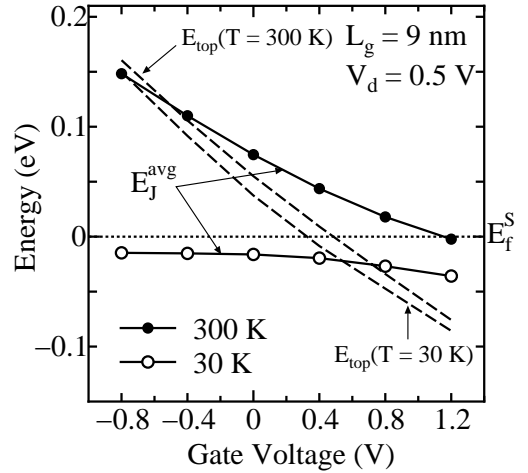


Figure 4: V_g dependence of E_J^{avg} and E_{top} at $T = 300$ K (closed circles) and at $T = 30$ K (open circles).

Acknowledgment

We would like to thank Semiconductor Technology Academic Research Center (STARC) for financial support.

References

- [1] H. Wakabayashi *et al.*, IEDM Tech. Dig., 429 (2004).
- [2] H. Takeda and N. Mori, Jpn. J. Appl. Phys. **44**, 2664 (2005).
- [3] A. Svizhenko *et al.*, IEEE Trans. Electron Devices **50**, 1459 (2003).
- [4] D.A. Antoniadis *et al.*, <http://www-mtl.mit.edu/researchgroups/Well/> (2001).
- [5] N. Mori *et al.*, Status Solidi (b) **204**, 268 (1997).
- [6] H. Takeda and N. Mori, to be unpublished in J. Comput. Electron.